The Solvent-Mode Effect on the Resonance Raman Excitation Profiles of Lycopene

Mineo SAITO and Yasushi MIKAMI*
Department of Chemistry, Faculty of Science, Tohoku University, Sendai 980
(Received August 6, 1985)

The solvent-induced broadening mechanisms are considered in the calculation of resonance Raman excitation profiles (RREP) for the ν_1 and ν_2 vibrational modes of lycopene. The broadening mechanisms are classified into two groups: Inhomogeneous broadening due to a distribution of the 0-0 transition energies and solvent-induced homogeneous broadening due to coupling with low-frequency solvent-solute interactions. The conventional sum-over-states formula for RREP is transformed to a formally equivalent expression in the time domain. The results show that the homogeneous broadening dominates the RREP of lycopene.

Recently, Cotting et al.[1] have analyzed the Raman lines of lycopene by using a model including both homogeneous and inhomogeneous broadening mechanisms as well as the multi-mode theory. They have assumed that each broadening is characterized by a Lorentzian distribution with a line width, either Γ (homogeneous) or $\Gamma_{\rm inh}$ (inhomogeneous). They have calculated the resonance Raman excitation profiles (RREP) for the ν_1, ν_2, and ν_3 Raman lines using various values of Γ and $\Gamma_{\rm inh}$, holding the total width $\Gamma_{\rm tot}$ ($=\Gamma+\Gamma_{\rm inh}$) constant at a value determined from the absorption spectra. At the values of $\Gamma_{\rm tot}$ ranging from 450 cm^{-1} to 500 cm^{-1}, with about a 75% (350 cm^{-1}) contribution from Γ, the theoretical excitation profiles are in good agreement with the experimental data measured in ethyl alcohol, toluene, and carbon disulfide solvents. These results are more informative than those calculated by Hokins[2] with only homogeneous broadening. Cotting et al.[1] do not explicitly refer to the origin of homogeneous broadening. However, 350 cm^{-1} seems to be too large for a realistic damping constant.

In this context, it is worthwhile to see how the interpretations of the damping constant in the RREP for β-carotene analogous to lycopene have changed in the last several years. Since Inagaki et al.[3] reported the experimental RREP of β-carotene, their broad band shapes have been questioned by many investigators. In earlier work, the phenomenological damping constant was used in explaining the broadness of the RREP. Siebrand et al.[4] took a value larger than 200 cm^{-1} as a damping constant to reproduce the experimental data. However, Kodama et al.[5] have pointed out that the large value is due not to the damping effect but mainly to the solvent (-solute) low-frequency modes, which are not Raman active. Ho et al.[6] have found the pure damping constant to be of the order of 50 cm^{-1}, considering both the damping and the low-frequency-mode effects. Further, Chan et al.[7] emphasized that low-frequency modes provide a Gaussian type of broadening.

We can expect that the damping constant in lycopene is similar to that of β-carotene. Thus, the low-frequency-mode effect should be included in analyzing the RREP of lycopene. In this article, we will investigate the RREP of lycopene by considering the low-frequency-mode effect as well as the homogeneous broadening with a rather small damping constant. Inhomogeneous broadening is also taken into account. This broadening is static in nature, reflecting the spread in molecular transition frequencies. Thus, the statistical distribution provides a Gaussian-type broadening, in contrast with the Lorentzian shape taken by Cotting et al.[1]

Theory

In order to analyze the band shapes of the absorption spectra and the RREP of lycopene, we make the following assumptions:

(a) The Condon approximation is used, since the π-π^* transition is strongly allowed.

(b) Only one component of the electronic-transition moments is nonzero.

(c) The displaced harmonic oscillator model is used for both intramolecular modes and solvent (-solute) low-frequency modes.

(d) The Einstein model is assumed for the solvent modes. Thus, these modes are reduced to one collective mode, whose frequency and displacement are given by $\omega_s=N^{-1}\sum\omega_k$ and $\Delta_s^2=N^{-1}\sum\Delta_k^2$ respectively, were N is the total number of the solvent modes and where k refers to an individual solvent mode.

(e) The distribution of 0-0 transition frequencies is responsible for the inhomogeneous broadening and has a Gaussian form, i.e.:

$$\rho_{\rm inh}(\omega)=(\sqrt{\ln 2})/\sqrt{\pi\Gamma_{\rm inh}^2}\,\exp[-(\omega-\omega_{0'0})^2\ln 2/\Gamma_{\rm inh}^2], \quad (1)$$

where $\omega_{0'0}$ is the mean value of the 0-0 transition frequencies and where $\Gamma_{\rm inh}$ is the inhomogeneous width.

The band-shape function of the absorption spectra of the system with inhomogeneous broadening is given by:

$$I(\omega_I)=\int d\omega\rho_{\rm inh}(\omega+\omega_I)I_h(\omega), \quad (2)$$

where ω_I is the frequency of the incident light and where $I_h(\omega)$ is the band-shape function without inhomogeneous broadening. Within the Condon approximation, we can separate $I_h(\omega)$ into the high-frequency part, $I_0(\omega)$, and the low-frequency part, $\rho_{\rm low}(\omega)$. Thus,

$$I_h(\omega)=|M_{ge}|^2\int d\omega' \rho_{low}(\omega')I_0(\omega'+\omega), \quad (3)$$

where M_{ge} is the electronic transition moment between the ground state (g) and the excited state (e). The high-frequency part, $I_0(\omega)$, represents the contribution from the optical modes which determine the intensity of the vibronic band. We can assume that the thermal excitation of the high-frequency modes can be neglected. Thus, the high-frequency part, $I_0(\omega)$, is given by:

$$\begin{aligned} I_0(\Omega) &= \frac{1}{\pi}\mathrm{Re}\sum_{v_1'=0}^{\infty}\cdots\sum_{v_n'=0}^{\infty}\prod_{j=1}^{n}|\langle 0|v_j'\rangle|^2\int_0^{\infty}dt\exp \\ &\quad [i(\Omega+\sum_{j=1}^{n}v_j'\omega_j)t-\Gamma t] \\ &= \frac{1}{\pi}\mathrm{Re}\int_0^{\infty}dt\prod_{j=1}^{n}\exp\left(-\frac{\Delta_j^2}{2}(1-e^{i\omega_j t})\right)\exp(i\Omega t-\Gamma t), \end{aligned} \quad (4)$$

where ω_j and v_j' are the vibrational frequency and the vibrational quantum number of the j-th mode in the excited state, and where Γ is the damping constant whose depenence on a vibrational level is neglected. The low-frequency part, $\rho_{low}(\omega')$, forms the band-shape function for the optical modes and is given by:

$$\rho_{low}(\omega')=\sum_{v_s=0}^{\infty}\sum_{v_s'=0}^{\infty}P_{v_s}|\langle v_s|v_s'\rangle|^2(v_s\omega_s-v_s'\omega_s-\omega') \quad (5)$$

where ω_s is a common vibrational frequency in the ground state and the excited state and where P_{v_s} the Boltzmann-distribution function of the v_s-th vibrational level in the ground state. $\rho_{low}(\omega')$ is also given by the following time integration:

$$\begin{aligned} \rho_{low}(\omega') &= \frac{1}{2\pi}\int_{-\infty}^{\infty}dt\exp\left(\frac{1}{2}\Delta_s^2(\langle n_s\rangle+1)e^{i\omega_s t}\right. \\ &\quad \left.+\frac{1}{2}\Delta_s^2\langle n_s\rangle e^{-i\omega_s t}-\frac{1}{2}\Delta_s^2(2\langle n_s\rangle+1)-i\omega' t\right) \end{aligned} \quad (6)$$

where $\langle n_s\rangle=(e^{h\omega_S/kT}-1)^{-1}$ is the thermal-average quantum number. We are concerned with the strong coupling case, i.e., $(1/2)\Delta_s^2(2\langle n_s\rangle+1)\gg 1$, in which the short time approximation used by Chan et al.[7] is valid. Thus, we can approximate $\rho_{low}(\omega')$ in this form:

$$\begin{aligned} \rho_{low}(\omega') &= \frac{1}{2\pi}\int_{-\infty}^{\infty}dt\exp\left(-it\left(-\frac{1}{2}\Delta_s^2\omega_s+\omega'\right)\right. \\ &\quad \left.-\frac{1}{4}\Delta_s^2(2\langle n_s\rangle+1)\omega_s^2 t^2\right) \\ &= (\sqrt{\ln 2}/\sqrt{\pi\Gamma_{low}^2})\exp[-(\omega'-\omega_{low})^2\ln 2/\Gamma_{low}^2], \end{aligned} \quad (7)$$

where $\omega_{low}=(1/2)\Delta_s^2\omega_s$ and where

$$\Gamma_{low}=\sqrt{\ln 2}\Delta_s\omega_s(2\langle n_s\rangle+1)^{1/2}. \quad (8)$$

Equation 7 indicates that the low-frequency mode induces a homogeneous broadening with a Gaussian shape with the width Γ_{low} and that the bodies of the absorption spectra are blue-shifted by ω_{low}. We call this broadening a "solvent-induced broadening."

By inserting Eq. 3 into Eq. 1, we obtain:

$$I(\omega_I)=|M_{ge}|^2\int d\omega\int d\omega'\rho_{inh}(\omega+\omega_I)\rho_{low}(\omega')I_0(\omega+\omega'). \quad (9)$$

Since both $\rho_{inh}(\omega+\omega_I)$, and $\rho_{low}(\omega')$ are Gaussian functions, their convolution is given by a Gaussian function:

$$I(\omega_I)=|M_{ge}|^2\int d\omega_a\rho_{tot}(\omega_a+\omega_I)I_0(\omega_a), \quad (10)$$

where:

$$\rho_{tot}(\Omega)=(\sqrt{\ln 2}/\sqrt{\pi\Gamma_{tot}^2})\exp[-(\Omega-\omega_{0'0}-\omega_{low})^2\ln 2/\Gamma_{tot}^2]$$

with $\Gamma_{tot}=\sqrt{\Gamma_{inh}^2+\Gamma_{low}^2}$. Only the total width, Γ_{tot}, can be obtained from the band shapes of the absorption spectra, so we cannot distinguish between inhomogeneous and solvent-induced homogeneous broadening. On the other hand, each broadening mechanism has a different influence on the band shapes of the RREP, as will be shown below.

The resonance Raman intensity of a fundamental line is given by:

$$S(\omega_I)\propto\omega_p^3\omega_I\int d\omega_a\rho_{inh}(\omega_a+\omega_I)\sum_{v_s=0}^{\infty}P_{v_s}|\alpha_{v_s}(\omega_a)|^2, \quad (11)$$

where ω_p is the frequency of the scattered light and where $\alpha_{v_s}(\omega_a)$ is the Raman tensor:

$$\begin{aligned} \alpha_{v_s}(\omega_a) &= -i(M_{ge})^2\sum_{v_1'=0}^{\infty}\cdots\sum_{v_n'=0}^{\infty}\int_0^{\infty}dt\langle 0|v_1'\rangle\langle v_1'|1\rangle e^{iv_1'\omega_1 t} \\ &\quad \times\prod_{j=2}^{n}|\langle 0|v_j\rangle|^2 e^{iv_j'\omega_j t}|\langle v_s|v_s'\rangle|^2 e^{i(v_s'-v_s)\omega_s t}e^{i\omega_a t-\Gamma t}. \end{aligned} \quad (12)$$

We can convert Eq. 12 into the analytic form, using the following relations:

$$\langle 0|v_j'\rangle\langle v_j'|1\rangle=\frac{\Delta_1}{\sqrt{2}}(1-e^{i\omega_1 t})\exp\left[-\frac{\Delta_1^2}{2}(1-e^{i\omega_1 t})\right], \quad (13)$$

$$|\langle 0|v_j'\rangle|^2 e^{iv_j'\omega_j t}=\exp\left[-\frac{\Delta_1^2}{2}(1-e^{i\omega_j t})\right] \quad (14)$$

and:

$$\begin{aligned} |\langle v_s|v_s'\rangle|^2 e^{i(v_s'-v_s)\omega_s t} &= \exp\left[-\frac{\Delta_s^2}{2}(1-e^{i\omega_s t})\right] \\ &\quad \times\sum_{p=0}^{v_s}\frac{v_s!\,e^{i(p-v_s)\omega_s t}}{p![(v_s-p)!]^2}\left(\frac{\Delta_s}{\sqrt{2}}(1-e^{i\omega_s t}-1)\right)^{2(v_s-p)}, \end{aligned} \quad (15)$$

where Δ_α (α=1, j, s) is the displacement of the α-th mode.

The lower-frequency part, Eq. 15, in Eq. 12 cannot be separated from the others, as in the case of absorption spectra, because the Boltzmann distribution factor, P_{v_s}, operates after $\alpha_{v_s}(\omega)$ is squared. The solvent-induced line-width, Γ_{low}, is related to the displacement, Δ_s, and the frequency, ω_s, of the low-frequency mode through Eq. 8. Thus, the solvent-induced line-broadening indirectly affects the RREP, though Γ_{low} does not explicitly appear in the formula. Fur-

ther, the RREP calculation clearly differentiates between the inhomogeneous broadening and the homogeneous broadening effects.

The time integrations in Eq. 4 and Eq. 12 can now be evaluated by the use of the time-dependent method proposed by Tannor and Heller.[9] In this article, the actual numerical integration is performed with the normalizing frequency, which has already been used in the calculation of radiationless transition rates in large molecules.[10,11] We now introduce the normalizing frequency, ω_N, which defines the integers:

$$\tilde{\omega}_j = \omega_j/\omega_N \text{ and } \tilde{\omega}_a = \omega_a/\omega_N.$$

Furthermore, the following quantities are defined:

$$\gamma = \Gamma/\omega_N \text{ and } x = \omega_N t.$$

Thus, we can write $I_0(\omega_a)$ in Eq. 9 as follows (see Eq. 4):

$$I_0(\omega_a) = \frac{1}{\pi\omega_N}\mathrm{Re}\sum_{v_1'=0}^{\infty}\cdots\sum_{v_n'=0}^{\infty}\prod_{j=1}^{n}|\langle 0|v_j'\rangle|^2 \times\int_0^{\infty}dx\exp(i\tilde{\omega}_a x+\sum_{j=1}^{n}iv_j'\tilde{\omega}_j x-\gamma x) \quad (16)$$

The time-integration in Eq. 16 leads to:

$$\int_0^{\infty}dx\exp(i\tilde{\omega}_a x+\sum_{j=1}^{n}iv_j'\tilde{\omega}_j x-\gamma x)=\frac{i}{\tilde{\omega}_a+\sum_{j=1}^{n}v_j'\tilde{\omega}_j+i\gamma} \quad (17)$$

On the other hand, we can easily obtain this relation:

$$\int_0^{2\pi}dx\exp\left(i\tilde{\omega}_a x+\sum_{j=1}^{n}v_j'\tilde{\omega}_j x-\gamma x\right)=\frac{i(1-e^{-2\pi\gamma})}{\tilde{\omega}_a+\sum_{j=1}^{n}v_j'\tilde{\omega}_j+i\gamma}. \quad (18)$$

because ω_j and ω_a are integers. Thus, we obtain:

$$I_0(\omega_a)=\frac{1}{\pi\omega_N(1-e^{-2\pi\gamma})}\sum_{v_1'=0}^{\infty}\cdots\sum_{v_n'=0}^{\infty}\prod_{j=1}^{n}|\langle 0|v_j\rangle|^2 \times\int_0^{2\pi}dx\exp(i\tilde{\omega}_a x+\sum_{j=1}^{n}iv_j'\omega_j x-\gamma x) =\frac{1}{\pi\omega_N(1-e^{-2\pi\gamma})}\int_0^{2\pi}dx\prod_{j=1}^{n}\exp\left[-\frac{\Delta_j^2}{2}(1-e^{i\tilde{\omega}_j x})\right]e^{i\tilde{\omega}_a x-\gamma x}. \quad (19)$$

Furthermore, we can replace the integration over the frequency in Eq. 10 by the following sum:

$$I(\omega_I)=\sum_{m=-\infty}^{\infty}\int_{m\omega_N}^{(m+1)\omega_N}d\omega_a\rho_{tot}(\omega_a+\omega_I)I_0(\omega_a) =\omega_N\sum_{m=-\infty}^{\infty}\rho_{tot}(m\omega_N+\omega_I)I_0(m\omega_N), \quad (20)$$

where we neglect the variation of the integrand in the $m\omega_N<\omega_a<(m+1)\omega_N$ region. A similar procedure leads to the following expressions for the resonance Raman intensity:

$$\alpha_{v_s}(\omega_a)=\frac{i}{\pi\omega(1-e^{-2\pi\gamma})}\int_0^{2\pi}dx\frac{1}{\sqrt{2}}(1-e^{i\omega_1 x}) \times\exp\left[-\frac{\Delta_1^2}{2}(1-e^{i\omega_1 x})\right] \times\prod_{j=2}^{n}\exp\left[-\frac{\Delta_1^2}{2}(1-e^{i\omega_j x})\right]\exp\left[-\frac{\Delta_s^2}{2}(1-e^{i\omega_s x})\right] \times\sum_{p=0}^{v_s}\frac{v_s!\,e^{i(p-v_s)\omega_s x}}{p![(v-p)!]^2}\left[\frac{\Delta_s^2}{2}(e^{i\omega_s x}-1)\right]^{2(v_s-p)} \quad (21)$$

and:

$$S(\omega_I)\propto\omega_p^3\omega_I\omega_N\sum_{m=-\infty}^{\infty}\rho_{inh}(m\omega_N+\omega_I)\sum_{v_s=0}^{\infty}P_{v_s}|\alpha_{v_s}(m\omega_N)|^2. \quad (22)$$

Results and Discussion

We will now analyze the band-shapes of the absorption spectrum and the RREP of lycopene in toluene solvents. The damping constant, Γ, is assumed to be $50\,cm^{-1}$ according to the case of β-carotene[6]; this corresponds to a picosecond relaxation process and seems to be realistic. This value has only a minor effect on the band-shapes of the absorption spectrum and the RREP, in the presense of inhomogeneous and solvent-induced homogeneous broadening mechanisms due to low-frequency modes.

The frequencies of the three Franck-Condon active modes, ν_1, ν_2, and ν_3, of lycopene are taken to be $\omega_1=1516\,cm^{-1}$, $\omega_2=1154\,cm^{-1}$, and $\omega_3=1005\,cm^{-1}$ respectively. The frequency, ω_s, and the displacement, Δ_s, of the solvent mode are related to the homogeneous line-width, Γ_{low}, through Eq. 8. In the following calculations, we first estimate the homogeneous line-width, Γ_{low}, from the absorption spectra. Thus, we do not need to provide ω_s and Δ_s independently. We prefer to give ω_s. Further, ω_s and Δ_s are somewhat arbitrary because only their combined quantity, i.e., Γ_{low}, is determined. Therefore, we can assume a round value of $50\,cm^{-1}$ as ω_s; this seems to be reasonable for an approximate frequency of the solvent mode. Let us now refer to the normalizing frequency, ω_N. For a given set of ω_j, a large number of ω_N values may give a value identical to those in Eqs. 19 and 21 because of the periodicity of the integrands. It is sufficient, however, to consider only their maximum- the largest common integer divider in the set. The value of ω_N should be, at most, $1\,cm^{-1}$ for our three ω_j values. However, even if some larger ω_N is used, the relative values of $\tilde{\omega}_j$ are not very largely altered, provided that each $\tilde{\omega}_j$ is redefined as the integer nearest to ω_j/ω_N. Therefore, we are allowed to adopt a larger ω_N than the largest common integer divider, disregarding a small rounding error. Thus, we take $25\,cm^{-1}$ as a value of ω_N. This value also satisfies the condition under which we can replace the integration into the sum in Eqs. 20 or 22, because the linewidth of lycopene is very large.

We adopt the same displacements of the three Franck-Condon active modes as those Cotting et al.[1] have used. Thus, we have $\Delta_1=1.1$, $\Delta_2=1.0$, and $\Delta_3=0.5$. Using these values of the displacements and varying the total width, Γ_{tot}, we calculate the absorp-

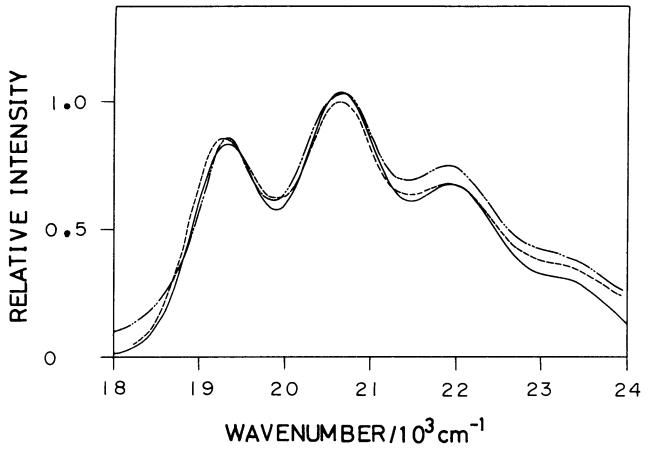

Fig. 1. Optical absorption line shapes for lycopene in toluene at 300 K. The measured absorption line shape (dashed line) is that of Ref. 1. The best fitted theoretical line shape (solid line) was obtained using Γ=50 cm^{-1} and Γ_{tot}=450 cm^{-1}, together with A_1=1.1, A_2=1.0, A_3=0.5 and $\omega_{0'0}+\omega_{low}$=19310 cm^{-1}. The (---) line is the another theoretical line shape with Γ=450 cm^{-1} and Γ_{tot}=0 cm^{-1}.

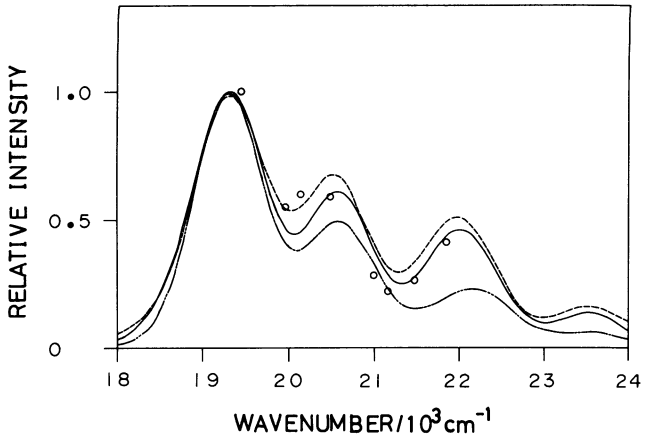

Fig. 2. Resonance Raman excitation profile line shapes of the ν_1 mode for lycopene in toluene at 300 K. The circles give a measured profile line shape of Ref. 1. The three theoretical curves are shown. The solid line is for Γ_{inh}=300 cm^{-1} and Γ_{low}=335 cm^{-1} the dashed line for Γ_{inh}=0 cm^{-1}, and Γ_{low}=450 cm^{-1} and the (---) line for Γ_{inh}=450 cm^{-1} and Γ_{low}=0 cm^{-1}. The other parameters used are the same as those in Fig. 1.

tion spectra and seek the curve best-fitting the experimental value. Figure 1 shows that the best fit is obtained at Γ_{tot}=450 cm^{-1} and $\omega_{0'0}+\omega_{low}$=19310 cm^{-1}. We also stress the good agreement in the lower-frequency region of the 0-0 band; this is in contrast to the result of Cotting et al. The disagreement may be due to a Lorentzian shape of the broadening. This fact is suggested by the following hypothetical calculations. We assume that only a pure damping effect contributes to the absorption band-width. That is to say, we take 450 cm^{-1} as the damping constant, Γ, and reduce Γ_{tot} to zero. The calculated absorbance comes to be higher than the one observed in the tail of the 0-0 band and resembles the result of Cotting et al. These results suggest that the main broadening mechanism is not related to the damping constant, Γ, giving a Lorentzian-type broadening, but to the width of inhomogeneous broadening, Γ_{inh}, and/or the width of the solvent-mode-induced broadening, Γ_{low}, both of which provide a Gaussian-type broadening.

In our model, Γ_{inh} and Γ_{low} cannot be distinguished in the analysis of the absorption spectra. On the other hand, the RREP calculation clearly differentiates between these effects, as has been shown in the previous section. First, we calculate the RREP for the two extreme cases. Figure 2 shows the RREP for the ν_1 vibrational mode of lycopene when only an inhomogeneous broadening exists and another extreme case in which only a homogeneous broadening mechanism is operative. The agreement between the theory and the experiment is better for the full homogeneous case than for the full inhomogeneous one. This fact suggests that the presence of low-frequency modes essentially determine the observed features of the RREP, in the case of the realistic damping constant, Γ, of 50 cm^{-1}. Further, a fairly large value (300 cm^{-1}) of inhomogeneous broadening Γ_{inh} only partly improves the RREP. This is intimately related to the Gaussian shape of homogeneous and inhomogeneous broadening. The total line-width for our Gaussian broadening is the same as that Cotting et al.[1] obtained by using the Lorentzian broadening mechanism. In the Lorentzian case, the total line-width, Γ_{tot}, is a sum of the inhomogeneous broadening, Γ_{inh}, and a damping constant, Γ. Since Γ_{tot} is determined to be constant from the absorption spectra, a large value of Γ_{inh} considerably reduces Γ. Cotting et al.[1] have already suggested that values of Γ_{inh} larger than 300 cm^{-1} may cause the major effect in the RREP. In our Gaussian case, however, the total line-width, Γ_{tot}, equals $\sqrt{\Gamma_{inh}^2+\Gamma_{low}^2}$. This relation leads to a still larger Γ_{low} (335 cm^{-1}), even at the large Γ_{inh} (300 cm^{-1}). The features of the RREP calculated with this Γ_{low} are similar to that of the full homogeneous case (Γ_{low}=450 cm^{-1}). In the presence of a large homogeneous broadening, an inhomogeneous broadening itself may little affect the RREP. A similar tendency is also shown for the ν_2 vibrational mode, as we can see in Fig. 3.

In conclusion, a reasonable damping constant, which is also similar to that of β-carotene, can be assumed for the case of lycopene if we take into account the solvent-induced broadening mechanisms. The full inhomogeneous broadening mechanism provides a rather large discrepancy between theory and experiment for the RREP. The experimental data are roughly consistent with the full homogeneous broadening mechanism. The effect of inhomogeneous

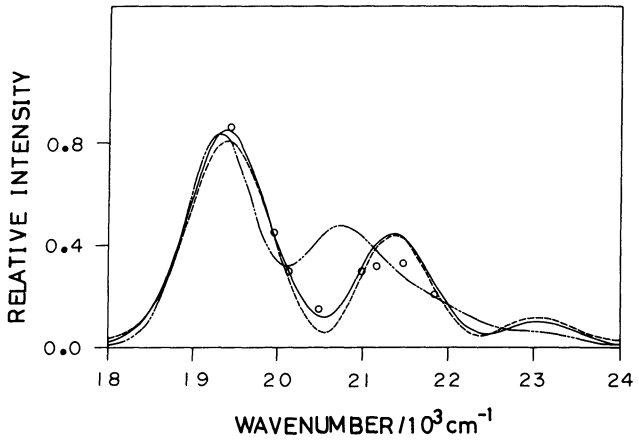

Fig. 3. Resonance Raman excitation profile line shapes of the ν_2 mode for lycopene in toluene at 300 K. The circles give a measured profile line shape of Ref. 1. The three theoretical curves are shown: The solid line is for Γ_{inh}=300 cm^{-1} and Γ_{low}=335 cm^{-1}, the dashed line for Γ_{inh}=0 cm^{-1}, and Γ_{low}=450 cm^{-1}, and the (---) line for Γ_{inh}=450 cm^{-1} and Γ_{low}=0 cm^{-1}. The other parameters used are the same as those in Fig. 1.

broadening partly improve the results, though the RREP values for the ν_1 and ν_2 vibrational modes of lycopene are insensitive to the large variation in Γ_{inh}.

The authors would like to thank Professor Takeshi Nakajima for his guidance and encouragement.

References

1) J. E. Cotting, L. C. Hoskins, and M. E. Levan, *J. Chem. Phys.*, **77**, 1081 (1982).
2) L. C. Hoskins, *J. Chem. Phys.*, **74**, 882 (1981).
3) F. Inagaki, M. Tasumi, and T. Miyazawa, *J. Mol. Spectrosc.*, **50**, 286 (1974).
4) W. Siebrand and M. Zgierski, *J. Chem. Phys.*, **71**, 3561 (1979).
5) K. Kodama and A. D. Bandrauk, *Chem. Phys. Lett.*, **80**, 248 (1981).
6) Z. Z. Ho, R. C. Hanson, and S. H. Lin, *J. Chem. Phys.*, **77**, 3414 (1982).
7) C. K. Chan and J. B. Page, *J. Chem. Phys.*, **79**, 5234 (1983).
8) Y. Toyozawa, "Dynamical Processes in Solid State Optics," R. Kubo and H. Kamimura, Benjamin, New York (1967), p. 90.
9) D. J. Tannor and E. J. Heller, *J. Chem. Phys.*, **77**, 202 (1982).
10) A. Nitzan and J. Jortner, *Theor. Chim. Acta*, **30**, 217 (1973).
11) Y. Mikami, *J. Chem. Phys.*, **73**, 3314 (1980).